



11-2-6

GROUND FAILURE EFFECTS ON PIPELINE SYSTEM PERFORMANCE

T. D. O'ROURKE¹, W. D. MEYERSONH¹, M. D. GRIGORIU¹, and M. M. KHATER¹

¹School of Civil and Environmental Engineering, Cornell University,
Ithaca, NY, USA

SUMMARY

A case study of the 1906 San Francisco earthquake shows that major losses in the San Francisco water supply resulted from: 1) surface faulting effects on buried pipelines, 2) severe shaking and deformation of pipeline bridges, and 3) buried pipeline response to liquefaction-induced lateral spreads. It further shows that pipeline system performance was affected severely by damage to a few critical lines. Methods for analyzing the effects of abrupt ground displacement on a buried ductile pipeline are reviewed. Principal pipe and soil properties affecting pipeline strain are combined in a dimensionless factor, referred to as the resistance index. Examples are given of how the resistance index can be used to predict pipeline strains in relation to the magnitude and geometry of ground deformation.

INTRODUCTION

This paper provides a brief review of the major pipeline failures during the 1906 San Francisco earthquake and traces their influence on system performance. Analytical methods for evaluating ductile pipeline response to fault movement are discussed. A dimensionless factor, referred to as the resistance index, is defined, in which principal soil and pipe properties are combined to estimate nonlinear pipeline response to ground rupture.

1906 SAN FRANCISCO EARTHQUAKE

The water supply of San Francisco is derived from two series of reservoirs which are interconnected by transmission pipelines and tunnels. South of San Francisco, water is impounded by earth and concrete dams to form the San Andreas, Crystal Springs, and Pilarcitos Reservoirs. Within the City of San Francisco, water is stored in a series of smaller reservoirs, from which it is conveyed through trunk lines into the main distribution network.

Figure 1 presents a plan view of the 1906 San Francisco water supply adapted from maps prepared by Schussler (Ref. 1). At the time of the earthquake, there was a combined volume of 88.7×10^9 liters in the San Andreas, Crystal Springs, and Pilarcitos Reservoirs. These reservoirs supplied nearly all water for the City of San Francisco in 1906, whereas today they represent approximately one-half of the local storage capacity in the San Francisco Bay Area. Superimposed on Fig. 1 are the approximate locations of pipeline damage

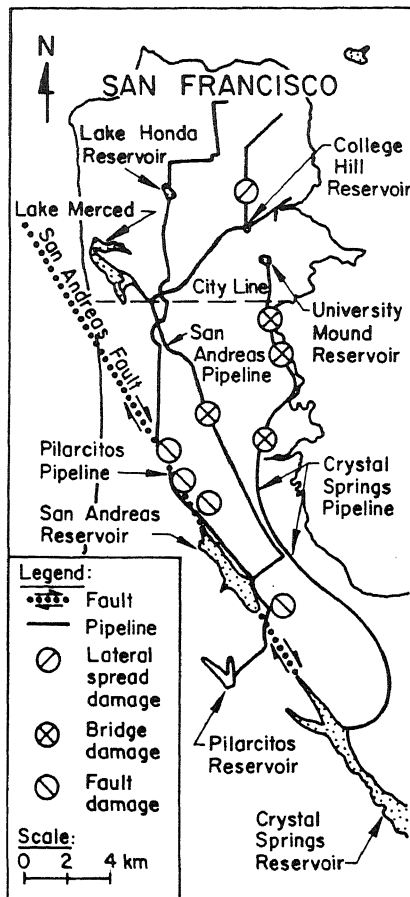


Fig. 1. Plan View of Damaged Water Supply

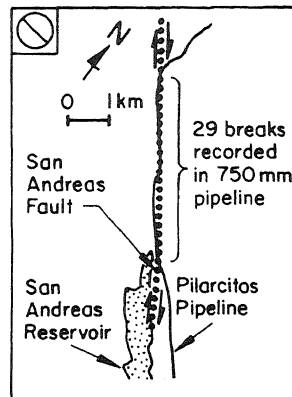


Fig. 2. Pipeline Damage from Fault Movement

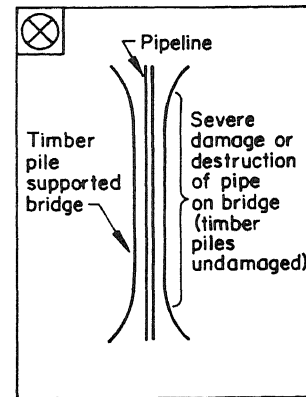


Fig. 3. Damage at Pipeline Bridge

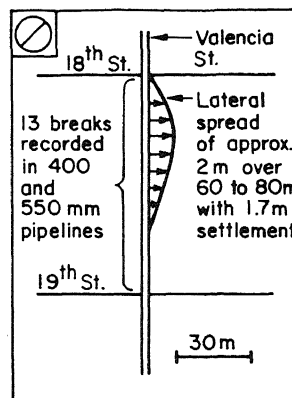


Fig. 4. Damage from Lateral Spread

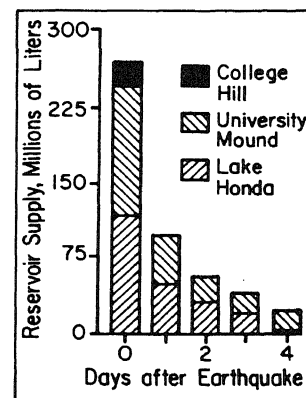


Fig. 5. Loss of Reservoir Storage

caused by the earthquake. There were three major causes of pipeline damage: 1) surface faulting, 2) severe dynamic distortion of pipeline bridges, and 3) lateral spreading of loose granular fill caused by soil liquefaction.

As illustrated in Fig. 2, right lateral strike-slip movement along the San Andreas fault was responsible for rupturing a 750-mm-diameter wrought iron pipeline conveying water from the Pilarcitos to Lake Honda Reservoir. Over 29 breaks were reported north of the San Andreas Reservoir, where the pipeline was constructed parallel to the San Andreas fault (Ref. 1). Fault movement near the San Andreas Reservoir was measured as 3.6 to 5.6 m (Ref. 2). Pipeline ruptures were caused by tensile and compressive deformation of the line. Over three months were required to reconstruct the pipeline.

As illustrated in Fig. 3, dynamic distortion of bridges was responsible for rupturing a 925-mm-diameter wrought iron pipeline conveying water from the San Andreas to College Hill Reservoir, and for rupturing at three swamp crossings an 1100-mm-diameter wrought iron pipeline conveying water from the Crystal Springs to University Mound Reservoir. The wooden trestle bridges all were damaged by strong ground shaking, with no damage or misalignment observed in their timber pile foundations. Approximately three days were required to repair

the 925-mm-diameter pipe, and over a month was required to restore the 1100-mm-diameter Crystal Springs Pipeline.

As illustrated in Fig. 4, two cast iron pipelines, 400 and 550 mm in diameter, were broken by liquefaction-induced lateral spreading and settlement across Valencia Street north of the College Hill Reservoir. These broken pipes emptied the reservoir of 4.3×10^7 liters, thereby depriving fire fighters of water for the burning Mission District of San Francisco. As indicated in previous studies (Ref. 3), this local deformation ranks as one of the most devastating events of the 1906 earthquake.

Figure 5 presents a bar graph showing the reservoir storage in San Francisco as a function of time after the earthquake. After four days, less than one-tenth of the initial capacity of the College Hill, University Mound, and Lake Honda Reservoirs was still available. Although water reserves were diminished to marginal levels, at no time was water lost throughout the entire system. Two factors were critically important in preserving flow. After pipeline repairs requiring 16 hours, water was pumped from Lake Merced into the Pilarcitos Pipeline to supply Lake Honda. This action provided an additional 2.6 to 3.0×10^7 liters/day, thereby maintaining capacity in Lake Honda for distribution to the northwestern parts of the city. After repairs of the San Andreas Pipeline over three days, approximately 3.0×10^7 liters/day were conveyed to the College Hill Reservoir for distribution in the South Mission area of the city. By the fourth day, approximately 6.0×10^7 liters of water were flowing into the city, in addition to the 2.5×10^7 liters still available in the reservoirs.

A review of the pipeline system performance during the 1906 San Francisco earthquake underscores the importance of local storage capacity within the city. All transmission pipelines supplying San Francisco were ruptured so that for three days, the water for post-earthquake fires was drawn entirely from reservoirs inside the city limits. System redundancy played a key role, in that water pumped from Lake Merced maintained flow into the northwestern distribution network.

Permanent ground movements and pipeline bridge damage were responsible for major losses in the system. Pipeline crossings of railways, highways, and water courses often involve support by special bridges or by transportation overpasses. These locations are potentially vulnerable to dynamic strains, as well as settlement of fill adjacent to the structures.

Ground ruptures from surface faulting and soil liquefaction represent a major source of potential damage. Because of their importance for system performance, analytical models for ground rupture effects on buried pipelines are examined in the following sections of this paper.

MODELS FOR PIPELINES CROSSING FAULTS

Many high pressure pipelines are constructed according to modern practices with continuous girth-welded steel sections of pipe. The inherent ductility of steel makes these types of pipelines well suited to sustain plastic strain if deformed in tension. Several models have been developed to account for ductile pipeline response to fault movement (Ref. 4). It should be recognized that such models are not necessarily confined to fault movement, but also can apply, in certain instances, to ground ruptures at the margins of lateral spreads or earthquake-induced landslides.

The model developed by Kennedy, et al. (Ref. 4) has been discussed extensively in the literature, and is used in this paper to illustrate some important

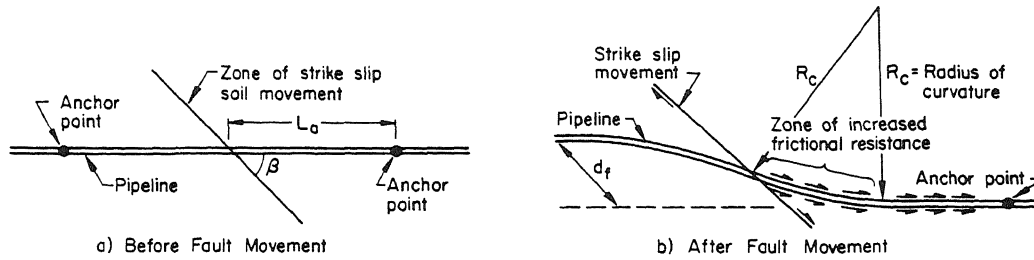


Fig. 6. Fault Crossing Model for Pipeline Analysis

characteristics of pipeline performance. As shown in Fig. 6, the model assumes that the pipeline is intersected by a fault at an angle, β , and subjected to tension. It is assumed that the pipeline is subjected to longitudinal frictional resistance through contact with the soil, and that the pipeline deforms in an antisymmetric pattern of two circular arcs. Anchors may be caused by bends, tie-ins, or other constraints which resist axial movement. Alternatively, the pipeline may be unanchored, in which case there is an effective anchor length, beyond which there is no axial stress imposed in the pipeline from fault movement. Kennedy, et al. (Ref. 4) assumed that the pipeline is subjected to increased axial friction in the zone of curvature near the fault. The radius of curvature is related to both the axial tension in the pipe and the lateral earth pressure mobilized against transverse movement of the pipe in the curved zone.

The maximum frictional resistance per unit pipe length, f , is evaluated by means of

$$f = \left(\frac{1 + K_0}{2} \right) \pi D \gamma H \tan \delta \quad (1)$$

in which γ is the unit soil weight, H is the depth to center of pipe, D is the external pipe diameter, K_0 is the coefficient of earth pressure at rest, and δ is the angle of shearing resistance mobilized between the pipeline and adjacent soil. In the zone of pipeline curvature near the fault, it is assumed that the frictional resistance is increased to values of $2.4 f$ and $3.3 f$ for depths of one and three times the pipe diameter, respectively.

The model uses a Ramberg-Osgood formulation (Ref. 4) to represent the non-linear stress-strain behavior of steel, in the form

$$\varepsilon = \frac{\sigma}{E_1} \left[1 + \frac{\alpha}{(r + 1)} \left(\frac{\sigma}{\sigma_0} \right)^r \right] \quad (2)$$

in which σ and ε are stress and strain, respectively, E_1 is Young's modulus, α and r are Ramberg-Osgood coefficients, and σ_0 is the effective yield stress of the steel.

In this paper, a dimensionless index, referred to as the resistance factor, R , is defined

$$R = \frac{f}{tE_p} \quad (3)$$

in which f is given by Eqn. (1), t is pipe wall thickness, and E_p is the modulus

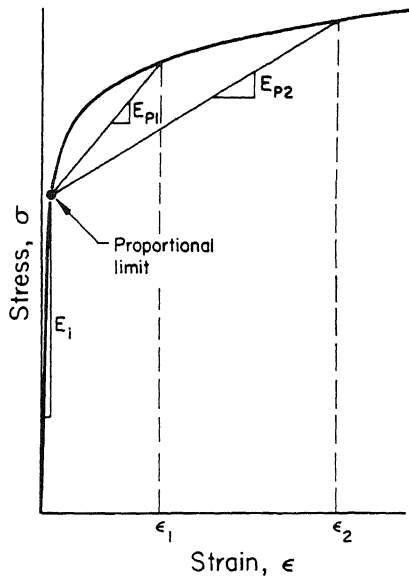


Fig. 7. Plastic Secant Modulus of Steel

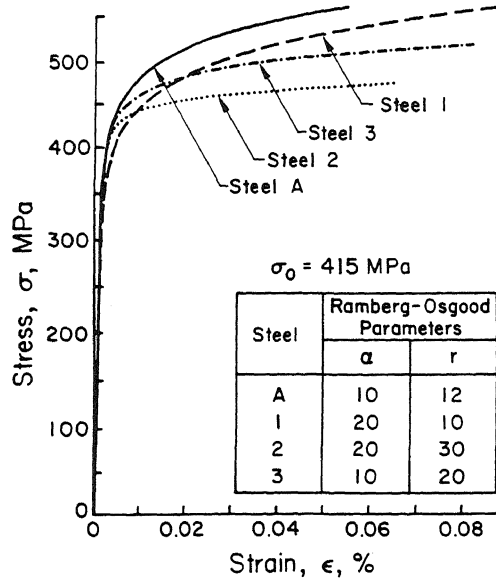


Fig. 8. Stress-Strain Plots for X-60 Steel

Note: Each analytical simulation represented by symbols: \diamond \circ \square

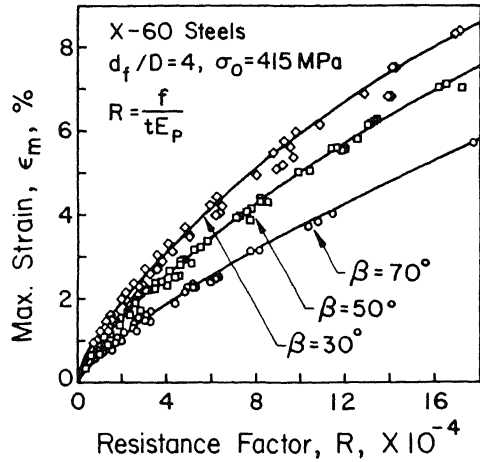


Fig. 9. Pipe Strain Vs. R, Const. d_f/D

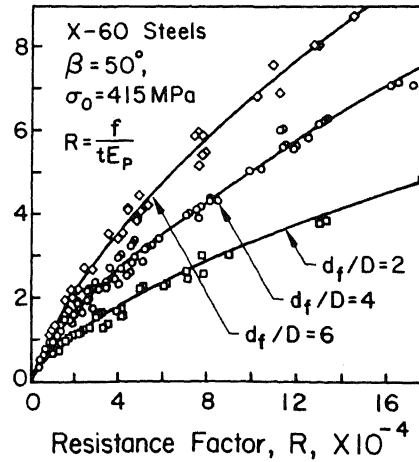


Fig. 10. Pipe Strain Vs. R, Const. β

as shown in Fig. 7. In essence, E_p is the secant modulus drawn from the proportional or linear limit to a point on the stress-strain curve of interest.

Several scores of analyses were run for X-60 steel, in which the pipe diameter and wall thickness, depth of burial, frictional resistance per unit pipe length, and stress-strain properties of the steel were varied. Figure 8 shows the four different stress-strain plots which were used and their associated Ramberg-Osgood parameters. A significant range of values was tested for each input parameter.

Figures 9 and 10 show the maximum pipeline strain from the analysis as a function of the R-factor for constant ratio of fault displacement to pipe diameter,

d_f/D , and angle of crossing, β , respectively. These results pertain to an unanchored pipeline. It can be seen that the R-factor acts to consolidate the analytical output into well-defined trends. This means that maximum strain estimates can be made for a variety of conditions, without resorting to analysis on a case-by-case basis. Moreover, the effect on pipeline strain of variations in the post-yield stress-strain relationship of the steel can be evaluated with relative ease. For this application, it should be recognized that E_p in the R-factor is defined for the same strain as given on the ordinate axis.

As an example, consider a 750-mm-diameter pipeline crossing a fault with $\beta = 50^\circ$, $t = 12.5$ mm, and $f = 22$ kN/m. The frictional resistance, f , in this case is consistent with a 1.2-m depth to centerline in medium dense sand. At a maximum strain of 0.04, E_p is 1.3 GPa and 3.3 GPa for Steel 2 and Steel A, respectively, as shown in Fig. 8. The R-factors for Steel A and Steel 2 are 5×10^{-4} and 13×10^{-4} , respectively. From Fig. 10, at a strain of 0.04, it can be seen that the maximum tolerable fault displacement decreases from 4.5 to 1.5 m, if Steel 2 is used instead of Steel A.

The analyses summarized in Fig. 10 indicate that the post-yield stress-strain relationship of steel can influence the tolerable amount of fault movement by a factor of as much as 3. In contrast, the pipeline strain imposed by large ground displacement is influenced to only a very small extent by yield strength. Because the post-yield modulus tends to decrease as the yield stress increases, the choice of higher grade steel may actually result in diminished capacity of the pipeline to accommodate the effects of ground deformation.

CONCLUSIONS

Severe losses were experienced in the 1906 San Francisco water supply as a result of buried pipeline rupture by fault movement and lateral spreading, and by dynamic distortion of pipeline bridges. Because the loss of a single pipeline can have a significant effect on system performance, models for the post-yield response of buried pipe to ground rupture can play an important role in strengthening and protecting water supplies and related pipeline systems. An R-factor is defined which combines the parameters of soil-pipe frictional resistance, wall thickness, and plastic modulus of the steel to provide an index of post-yield pipeline response to abrupt ground deformation.

ACKNOWLEDGMENTS

The authors thank the National Center for Earthquake Engineering Research and the National Science Foundation for sponsoring research under Grant No. 873007, from which this paper was prepared.

REFERENCES

1. Schussler, H., The Water Supply of San Francisco, California, Spring Valley Water Company, (1906).
2. Lawson, et al., The California Earthquake of April 18, 1906, Carnegie Institution of Washington, (1908).
3. O'Rourke, T. D. and Lane, P. A., "A Case Study of Seismic Hazards and Pipeline System Response for San Francisco," 3rd U. S. National Conference on Earthquake Engineering, 3, 2167-2178, (1986).
4. Kennedy, R. P., Chow, A. W., and Williamson, R. A., "Fault Movement Effects on Buried Oil Pipeline," Journal of the Transportation Engineering Division, ASCE, 103, TE5, 617-633, (1977).